# Photovoltaic materials – present efficiencies and future challenges

Albert Polman[1], Mark Knight[1], Erik C. Garnett[1], Bruno Ehrler[1], and Wim C. Sinke[1,2]

[1]Center for Nanophotonics, FOM Institute AMOLF
Science Park 104, 1098 XG Amsterdam, the Netherlands

[2]Energy research Center of the Netherlands (ECN)
P.O. Box 1, Petten, the Netherlands

**The development of photovoltaic materials has seen a spectacular growth in the recent past. We review the electrical characteristics of record cells of 16 widely studied photovoltaic materials geometries (efficiencies 10-29%) and compare these to the fundamental limits based on the Shockley-Queisser detailed-balance model. Based on this analysis, we derive the key limiting factors and future challenges for these solar cell materials related to efficient light management and charge carrier collection. Prospects for practical application and large-area fabrication, for which achieving high efficiency is a key factor, are discussed for all materials.**

## 1. Introduction

Photovoltaics (PV), which directly convert solar energy into electricity, offer a practical and sustainable solution to the challenge of covering the increasing global energy demand. The price of PV systems has dramatically decreased in the past years and the levelized cost of electricity of PV can now compete with the variable portion of consumer electricity prices in many countries worldwide: the point of "socket parity" has been reached (*1*). Substantial further cost reduction is needed, however, to allow PV to compete in more electricity markets and to enter the multi-terawatt regime. Aside from the solar cell and module fabrication costs, a major and increasing fraction (now typically 50%) of the cost of PV generation is related to PV system components and installation: inverters, cabling, mounting structures, labor, etc. (*1*). As a result, solar cell efficiency is a key lever for PV cost reduction: for a given output power a higher cell efficiency directly translates into a smaller and therefore less expensive PV system, reducing the levelized cost of electricity. A higher power generation rate per unit area is also important in urban environments where space is limited. The development of photovoltaic materials is experiencing an enormous growth and efficiency records are continuously broken. In this Review we systematically compare the state-of-the-art of the 16 most studied PV materials geometries with particular emphasis on the limitations of each material and its potential for further improvements and large-scale application.

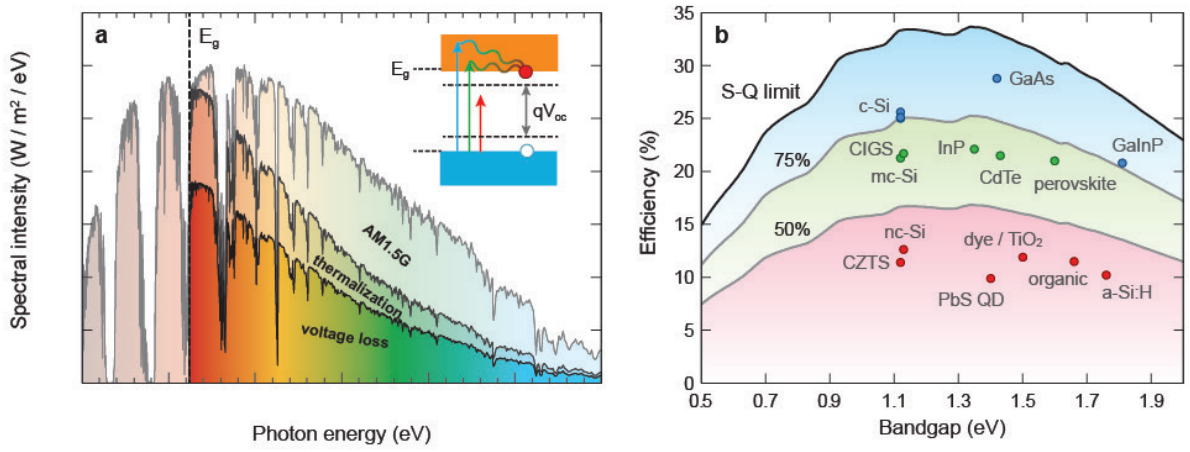


**Figure 1 | Fundamental solar cell efficiency limits and present-day records. a**. AM1.5 solar spectrum with distinct dips due to molecular absorption in the earth's atmosphere. Photons with energies below the band gap ($E_g$, dashed black line corresponds to the band gap of Si) are not absorbed, while photons with energies above the band gap are not fully converted to electrical energy due to thermalization of charge carriers. The maximum power generated by the cell is limited by voltage loss relative to the band gap voltage. *Inset*: electronic band structure with the separation of the quasi-Fermi levels determining the open circuit voltage $V_{oc}$. **b**. Theoretical Shockley-Queisser detailed-balance efficiency limit as a function of band gap (black line), and 75% and 50% of the limit (grey lines). The record efficiencies for different materials are plotted for the corresponding band gaps.

Solar cells are made of semiconductor material and, given the broad solar spectrum, their fundamental efficiency limit is determined by several factors (Fig. 1). Photons with energies below the band gap are not absorbed, while photons with energies above the band gap are not fully converted to electrical energy due to thermalization of charge carriers (inset in Fig. 1a). Taking these two factors into account, ~45% of the incident spectrum-integrated solar power remains for semiconductors with a band gap of 1.1-1.4 eV. This is the maximum power that would be generated if the cell were operated at a voltage corresponding to the band gap energy and a current corresponding to full capture of all photons with energy above the band gap, followed by full collection of all generated carriers.

Even in an ideal case, however, the open-circuit voltage $V_{oc}$ is always lower than the band gap energy since thermodynamic detailed balance requires the cell to be in equilibrium with its environment, which implies that there is spontaneous light emission from the cell. The corresponding radiative carrier recombination represents a dark current that causes $V_{oc}$ to be well below the band gap voltage $V_g$ (inset in Fig. 1a). Furthermore, under maximum-power operation (at maximum $J \times V$) the voltage $V_{mp}$ is lower than $V_{oc}$ and the current density $J_{mp}$ is lower than the maximum (short-circuit) current density $J_{sc}$ (inset in Fig. 2a). The efficiency limit that takes all these factors into account was first derived by Shockley and Queisser (S-Q) in 1961 (*2*). Figure 1b shows this limiting efficiency for a single-junction solar cell under "one-sun" illumination with the standard AM1.5 solar spectrum

as a function of band gap; the maximum efficiency occurs for a semiconductor with bandgap of 1.34 eV and is 33.7%.

In practical solar cells not all incident light is absorbed in the active layer(s) and not all generated carriers are collected, lowering $J_{sc}$ below the maximum value that can be achieved for a given band gap, $E_g$. Also, Auger recombination, band tail recombination, and recombination at bulk, interface and surface defects reduce the achievable $V_{oc}$ below the S-Q value (*3-5*). Furthermore, resistance and contact losses and other non-idealities reduce the fill factor, $FF=(V_{mp}J_{mp})/(V_{oc}J_{sc})$. Combined, these factors lead to practical efficiencies that are - often substantially - lower than the S-Q limit for a given band gap.

**2. Ideal and record solar cells compared**

In this review we distinguish three photovoltaic materials classes:

(1) ultra-high efficiency monocrystalline materials with efficiencies >75% of the S-Q limit for the corresponding band gap: Si (homojunction and heterojunction), GaAs, and GaInP;

(2) high-efficiency multi- and polycrystalline materials (50-75% of S-Q limit): Si, $Cu(In,Ga)(Se,S)_2$ ("CIGS"), CdTe, methyl-ammonium-lead-halide perovskite ($CH_3NH_3Pd(I,Cl,Br)_3$); and InP;

(3) low-efficiency materials (<50% of S-Q limit): micro/nanocrystalline and amorphous Si, $Cu(Zn,Sn)(Se,S)_2$ ("CZTS"), dye-sensitized $TiO_2$, organic/polymer materials, and quantum dot materials.

The record efficiency for each of these materials (see also Supplementary Materials, Table S1) is plotted in Fig. 1b. The experimental values for $J_{sc}$, $V_{oc}$, and *FF* for the record-efficiency cell reported for each individual material are plotted in Fig. 2a-c, together with the limiting values calculated using the S-Q model (*2*). The experimental values for $J_{sc}$ generally follow the trend given by the S-Q limit, with some materials closely approaching this limit. Values for $V_{oc}$ and *FF* are much more scattered with only a few materials approaching the S-Q limit. To analyze these trends we evaluate two characteristic parameters: (1) the current ratio $j=J_{sc}/J_{SQ}$ which is a measure for the degree of light coupling, absorption, and trapping in the active layer(s) of the cell, and also depends on the carrier-collection efficiency; and (2) the voltage ratio $v=V_{oc}/V_{SQ}$ which is primarily related to the degree of recombination of carriers in the bulk, surfaces and interfaces. Together, the voltage ratio *v* and fill factor ratio $f=FF/FF_{SQ}$ indicate the total electrical limitations of a cell (*6*). Figure 3 plots *j* versus $v \times f$ for all evaluated materials, and directly indicates to what degree the cell efficiency is limited by light management or charge-carrier management. Next, we describe these data for all materials.

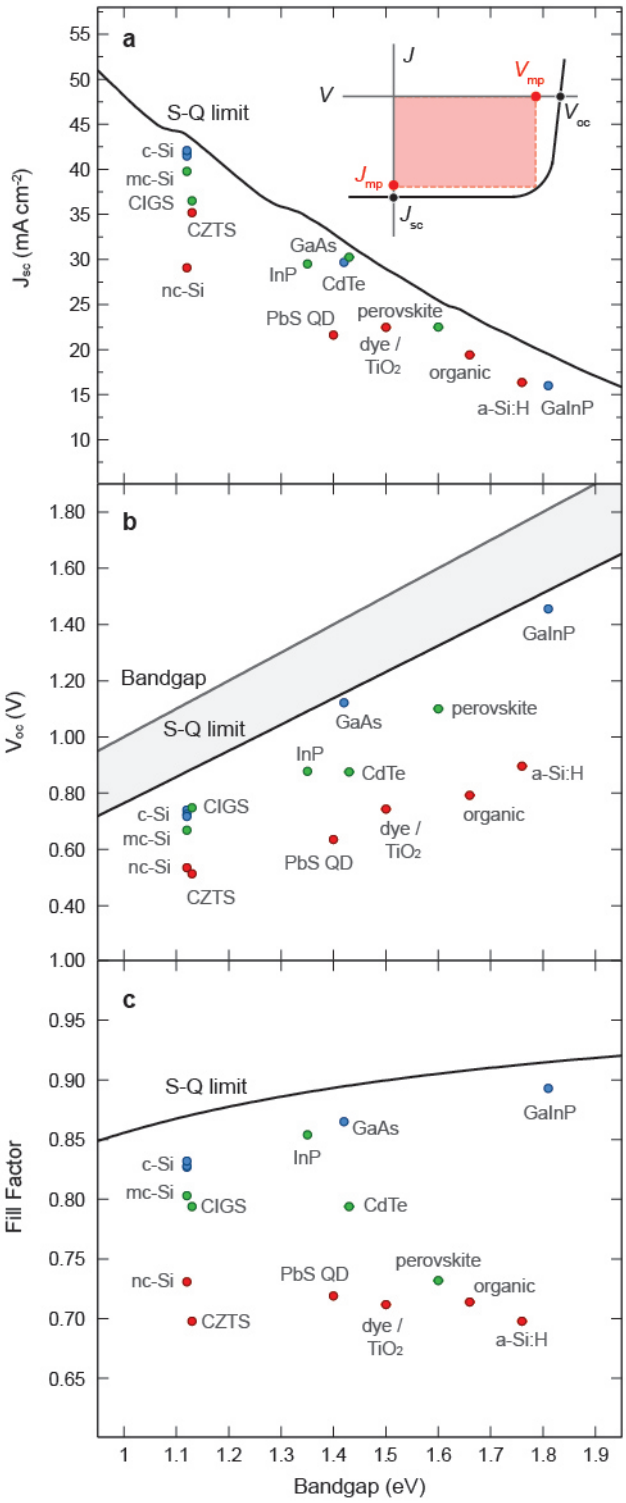


**Figure 2 | Record cell parameters compared to the detailed-balance limit.** Single-junction solar cell parameters as a function of band gap energy according to the Shockley-Queisser limit (solid lines) and experimental values for record-efficiency cells. **a**. Short-circuit current $J_{sc}$. Inset: a typical current-voltage $J(V)$ curve, with $V_{oc}$, $J_{sc}$, $V_{mp}$, and $J_{mp}$ indicated. The product of current and voltage is highest at the maximum power point ($J_{mp}V_{mp}$). **b**. Open-circuit voltage $V_{oc}$. The voltage corresponding to the band gap is shown for reference, with the voltage gap $V_g$-$V_{SQ}$ indicated by the gray shaded region. **c**. Fill factor $FF=(J_{mp}V_{mp})/(V_{oc}J_{sc})$. All data are for standard AM1.5 illumination at 1000 W/m$^2$.

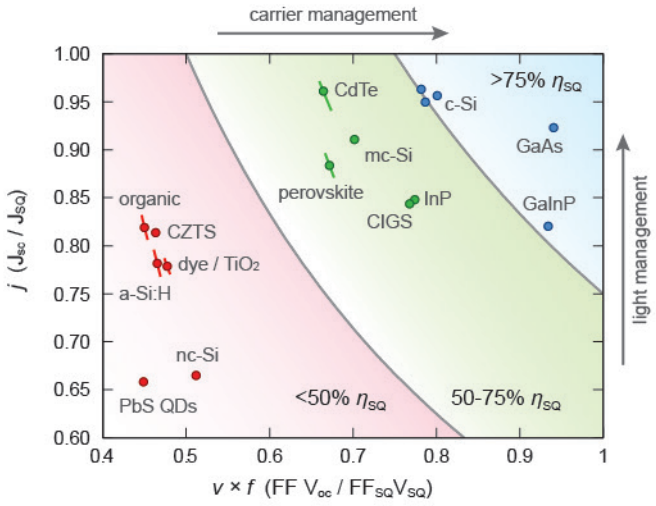


**Figure 3 | Fraction of Shockley-Queisser detailed-balance limit for voltage and current achieved by record cells.** The current ratio $j = J_{sc}/J_{SQ}$ is plotted versus the product of the voltage and fill factor fractions ($v \times f = V_{oc}FF/V_{SQ}FF_{SQ}$) for the record-efficiency cells of all evaluated materials. The lines around some data points correspond to a range of band gaps taken in the S-Q calculations according to uncertainty in the band gap of the record cell. Arrows on top and right axes indicate how improved light management and charge carrier collection improve the cell efficiency.

***Silicon (25.0-25.6%)***

Silicon has a nearly ideal band gap ($E_g$=1.12 eV) to reach high efficiency (Fig. 1). Si homojunction cells are based on a *p*-*n* junction made into either *p*-type or *n*-type Si(100) substrates. Several advanced device architectures and contacting schemes have been developed for Si solar cells. Contact recombination represents a major source of loss, so the most successful approaches either minimize contact area (*e.g.* by localized heavy doping or metal deposition), implement passivated contacts, or use a combination of these approaches. In parallel, surface passivation of Si using *e.g.* $Si_3N_4$, $Al_2O_3$, $SiO_2$ or combinations of these materials has been developed to great perfection. The record efficiency for a monocrystalline Si homojunction cell has recently been set at 25.1% (*7*) for a cell with a full-area tunnel-oxide passivated rear contact and high-quality top surface passivation (the TOPCon design, see Fig. 4a), slightly higher than the record value of 25.0% that stood since 1998 (*8, 9*) for a cell utilizing local contacts and high-quality surface passivation (the Passivated Emitter Rear Localized diffused (PERL) design).

The new record cell has excellent current generation and collection (*j*=0.96); similar to the value achieved for the two other record Si solar cell designs (see Table S1). This results from a combination of very low surface reflection achieved by a pyramidal (111)-faceted surface texture combined with an anti-reflection coating, and very low recombination losses in the silicon wafer and at the surfaces and contact interfaces. Low recombination is also reflected in the relatively high voltage of the record TOPCon cell (*v*=0.82).

In a radically different design, both the p-n junction and the contacts are placed at the rear of the cell. This interdigitated back-contact (IBC) design features alternating p-type and n-type contact regions (Fig. 4b). The IBC design eliminates front contact shading losses and reduces series resistance

by allowing more metal to be used for current collection and transport. This comes at the cost of more challenging carrier transport in the device (carriers generated near the surface must be collected at the back) and requires very-high-quality material to be used. Overall current generation and collection in the IBC cell is slightly lower than in the TOPCon cell (*j*=0.95 *vs* 0.96), as is the record efficiency (25.0% *vs* 25.1%) (*9-11*). It is noted that the record IBC cell has an area of 120 $cm^2$, while the TOPCon cell measures 4 $cm^2$. The record IBC cell uses a doped surface layer that creates a front surface field that repels carriers from the surface and has a $Si_3N_4$ top layer that serves both as an antireflection coating (ARC) and a high-quality passivation layer for the Si surface. The lower surface and bulk recombination rates lead to a slightly higher voltage (*v*=0.83) for the IBC cell compared to the TOPCon cell.

An efficiency record of 25.6% was recently reported for an IBC Si solar cell employing silicon heterojunctions (SHJ) for carrier collection instead of homojunctions (*9, 12*). In this approach, a thin stack of doped and intrinsic hydrogenated amorphous Si (a-Si:H) layers is deposited onto a crystalline silicon surface to form a junction, replacing the process of junction formation by high-temperature dopant diffusion (Fig. 4c). The SHJ design avoids carrier recombination in highly doped p-type and n-type regions and is made using a low-temperature process, which better preserves the minority carrier lifetime of the Si wafer. The surface of the record SHJ cell is passivated with a-Si:H. Altogether, this design led to the highest voltage observed for a Si solar cell (*v*=0.84). The overall result of carrier generation and collection is similar to that of the TOPCon cell (*j*=0.96). The origins of the small remaining losses in these high-efficiency Si cells are quite different, due to their different design and mode of operation.

Due to the indirect band gap of Si the absorption coefficient is relatively low and varies only gradually around the band gap energy so that a relatively thick wafer is required to absorb all light with photon energies above the band gap. This, however, leads to higher bulk (Auger) recombination and thus reduces $V_{oc}$. Moreover, it increases the materials costs. The tradeoff between cost, manufacturability and performance currently leads to an optimum Si wafer thickness of 100-200 μm for commercial cells. These wafers are made by diamond wire sawing from monocrystalline Si rods produced by Czochralski crystal growth.

Multicrystalline Si wafers are cut from cast ingots produced using directional, unseeded or seeded, crystallization, and have lower fabrication costs than monocrystalline wafers. The typical grain size depends on the growth method and can be as large as several centimeters. Multicrystalline Si has a lower electronic quality due to crystal grain boundaries and intra-grain defects, and a higher concentration of impurities. As a result, the record multicrystalline Si cell has high voltage loss (*v*=0.76). Light trapping in these cells is less efficient since the ideal pyramidal surface texture normally formed by alkaline etching Si (100) to the (111) surface facets cannot be realized on a

multicrystalline surface. This, together with incomplete carrier collection due to recombination leads to a reduced current ($j$=0.91) Together, these voltage and current losses lead to a lower efficiency (21.3%) (*9, 13*) than for monocrystalline Si cells. The record multicrystalline Si cell has a PERC p-n junction design with a tri-layer $SiO_2$/a-Si:H/$Si_3N_4$ ARC and passivation coating (Fig. 4d).

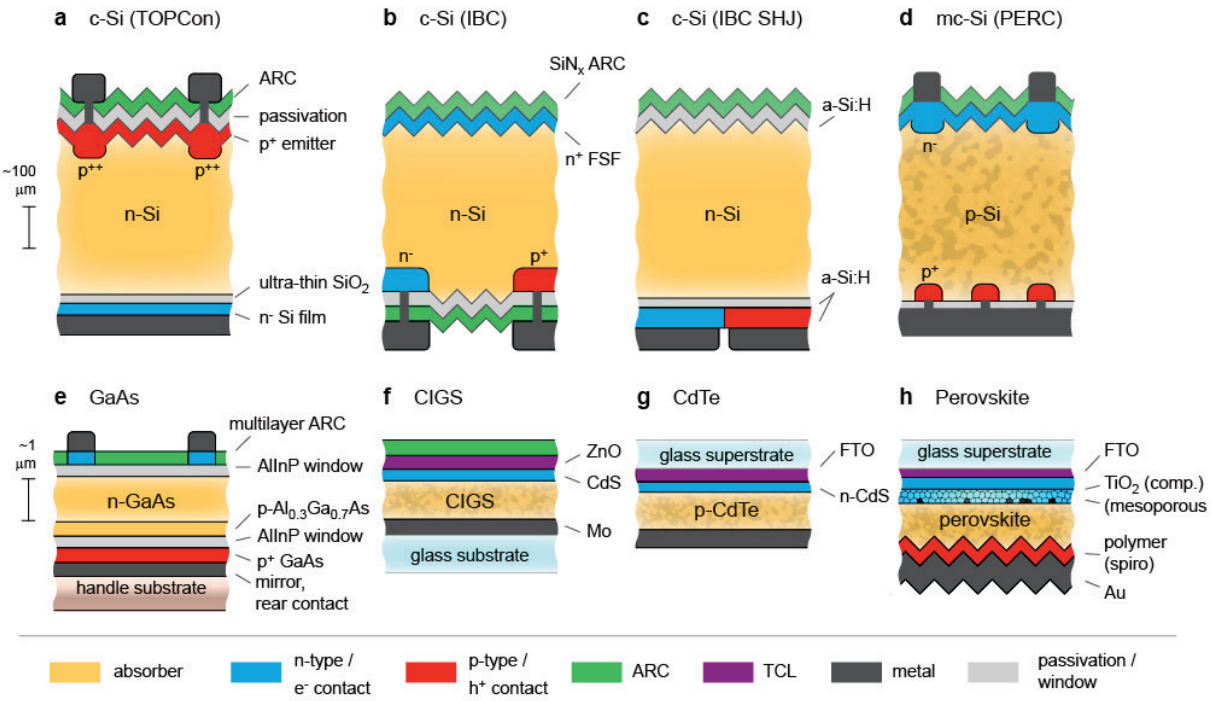


**Figure 4 | Layer and contact geometry for solar cells with record efficiency above 20%. a**. 25.1% TOPCon crystalline Si (Fraunhofer). **b**. 25.0% IBC crystalline Si (SunPower). **c**, 25.6% heterojunction IBC crystalline Si (Panasonic). **d**. 21.3% multicrystalline Si (Trina Solar). **e**. 28.8% GaAs thin film (Alta Devices). **f**. 21.7% CIGS thin film (ZSW Stuttgart). **g**. 21.0% CdTe thin film (First Solar). **h**. 20.1% perovskite thin film (KRICT).

According to the S-Q model, the efficiency limit for Si solar cells is 33.3%, far above the experimental record of 25.6%. A key limiting factor that is not accounted for in the S-Q model is Auger recombination of free carriers that occurs under illumination. Taking this into account for silicon, the efficiency limit for an undoped (monocrystalline) Si cell with optimized thickness (110 µm) was calculated to be 29.4% (*14*), leaving significant room for further development of existing technologies in the coming years.

Today, the global PV market is dominated by wafer-based crystalline silicon solar modules, with a total market share of over 90%. Within this, monocrystalline silicon covers ~35% and multicrystalline silicon ~65% (*15*). PV systems based on Si solar cells installed in the field have proven high reliability and very limited efficiency degradation over a period longer than 25 years.

***GaAs (28.8%)***

The record efficiency for a single-junction solar cell under one-sun illumination has been achieved using GaAs (28.8%) (*9, 16*). This material has a direct band gap close to the optimum (1.42 eV; Fig. 1). Because of the high optical absorption coefficient of GaAs the cell thickness can be kept relatively small (~2 μm) to harvest the solar spectrum up to the band gap. The record cell design has a n-GaAs/p-$Al_{0.3}Ga_{0.7}As$ junction geometry with high-bandgap window layers that serve to retain minority carriers in the GaAs active layer (Fig. 4e). The GaAs heterostructure is epitaxially grown using chemical vapor deposition, which is a relatively energy-intensive process. Interestingly, the record cell efficiency was achieved using a lift-off process, in which a ~2 μm thick GaAs foil was exfoliated from the substrate by chemical etching of an AlAs buffer layer, and laminated onto a Cu substrate. The voltage of the record cell is very high (*v*=0.97). Light reflection, top-finger shadowing, incomplete light trapping, and absorption in the metal back contact result in some current loss (*j*=0.92), leaving room for improvement. Application of an IBC geometry, for example, could potentially further increase *j*. An intermediate dielectric back-reflecting geometry can reduce parasitic absorption in the metal back contact. The fill factor in these cells is very high (*f = 0.97*). Taking into account Auger recombination, the maximum efficiency that can be achieved for a practical single-junction GaAs cell is ~32% (*17*), significantly above the current record value.

While III-V solar cells have traditionally been used in niche markets requiring high efficiency on a small area, such as space technology, the newly developed layer-transfer technology enables fabrication of large-area flexible (single-junction) GaAs technology at reduced costs for a much broader range of applications. Encapsulation and recycling of commercial GaAs modules is important because of the use of the toxic element As.

***InP (22.1%) and GaInP (20.8%)***

Two other III-V compound semiconductors that have achieved high efficiencies are InP and GaInP. InP ($E_g$ = 1.35 eV) has a band gap similar to GaAs, but the maximum reported efficiency of 22.1% (*9, 19*) is much lower than for GaAs, due to both lower voltage and current (*v*=0.81, *j*=0.85). Because of the existing high-efficiency GaAs alternative and the scarcity and associated high costs of In developments on InP cells have been minimal in the last decade. GaInP has a relatively high band gap (1.81 eV), for which the S-Q limit efficiency is 25.2%. The record efficiency that was achieved for GaInP cell is 20.8% (*9, 20*). The voltage loss on the record cell is extremely small (*v*=0.96), while current collection (*j*=0.82) in these cells leaves much room for improvement. The record GaInP cell has the highest fill factor achieved for any material (*FF*=0.89; *f*=0.98), which is partly related to the high band gap (Fig. 2c). Due to its large band gap GaInP is used in III-V multijunction solar cell

geometries, such as described above. Recently, a mechanically stacked tandem composed of a GaInP top cell and a Si heterojunction base cell was reported with an efficiency of 29.8% (*11, 21*).

***CIGS (21.7%)***

The record efficiency of $Cu(In,Ga)(Se,S)_2$ ("CIGS") thin-film solar cells has steadily increased over the past 20 years, with the present record value at 21.7% (*9, 22*), making it the highest-efficiency thin-film solar cell material to date (very closely followed by CdTe: 21.5% (*9, 23*)). CIGS has a chalcopyrite crystal structure and its band gap can be continuously tuned between about 1.0 and 2.4 eV by varying the In/Ga and Se/S ratios, with the low-bandgap compositions so far always giving the best performance. Polycrystalline films of CIGS are made using sputtering or evaporation from the constituent elements and are typically deposited onto a Mo film that is sputtered on a sodalime glass substrate. The typical active layer thickness is ~2-3 μm. Sodium diffusing from the glass substrate into the CIGS layer has been found to play a key role in passivating defects in the CIGS layer; the record cell also incorporated traces of K. The CIGS composition is typically graded to form an electric field that repels minority carriers from the Mo back contact, which is a strong recombination sink. The cell is finalized by the chemical-bath deposition of CdS to form a heterojunction followed by an intrinsic ZnO buffer layer, a transparent conducting layer (TCL) (ZnO:Al) and a $MgF_2$ ARC (Fig. 4f). In some recent high-efficiency devices the CdS layer is replaced by the more transparent $ZnO_xS_{1-x}$. Indium is a key element in CIGS and its scarcityis a concern for scaling up CIGS module production to the TW level.

The voltage for the record CIGS cells ($E_g$=1.13 eV) is very high, with $v$=0.84, equal to the best monocrystalline Si cells. Given the polycrystalline nature of the material, this implies that grain boundaries in this material do not act as strong carrier recombination sites. There is substantial current loss ($j$=0.84) due to light reflection, incomplete light trapping, absorption in the Mo back contact, and parasitic absorption in the CdS and ZnO:Al layers. The absorption spectrum of CIGS shows a rather gradual variation with energy around the band gap, which leads to unavoidable current loss in the near-bandgap spectral range. As with all polycrystalline materials, improving material quality is a complex process that requires optimization of many different parameters such as deposition conditions, (post-)annealing procedures and ambients. Due to the complex stoichiometry of CIGS, many secondary phases are possible and much of the progress in efficiency has been achieved by optimizing the deposition and annealing process to avoid such detrimental by-products. Creating a good Ohmic electrical contact between Mo and CIGS (via a $MoSe_2$ interfacial layer) is another important factor. Replacing the CdS buffer layer with a non-toxic and more transparent material is also a key research area.

The possibility of bandgap-tuning makes CIGS an interesting material in tandem solar cells either by combining CIGS layers with different band gaps, or using a high-bandgap CIGS top cell on top of a Si base cell. So far, however, high-bandgap (Ga-rich) CIGS cells have not yielded sufficient efficiencies for a CIGS/Si tandem to beat the record Si cell.

***CdTe (21.5%)***

CdTe is a binary semiconductor with a cubic zincblende crystal structure and a near-ideal band gap of 1.43 eV. It can be deposited at relatively low temperature using evaporation from CdTe powder. Cells are typically grown in a superstrate configuration starting from a glass substrate coated with fluorine-doped tin oxide (FTO). The subsequent layer stack usually consists of CdS (generally deposited by chemical bath deposition), followed by evaporated CdTe (thickness typically 2-3 μm) and a metal back contact such as Al or Ti, in some cases with a CuZnTe interfacial layer between the metal and the CdTe (Fig. 4g).

The highest reported certified efficiency for CdTe is 21.5% (*9, 23*), although for the purpose of this review we analyze cells with the previous record of 21.0% (*24*), as detailed data for the new record cell are not yet available. The steep absorption coefficient versus energy for CdTe enables very good current collection in CdTe cells ($j$=0.96), far superior to any other thin-film technology and equal to that of the record monocrystalline silicon cells. Voltage loss in CdTe cells is high ($v$=0.75) which is attributed to recombination losses in the crystal grains and at interfaces in the polycrystalline material, of which the exact nature is still unclear.

CdTe solar modules are commercially produced by several companies and presently have the largest market share among the thin-film technologies, which are dominated by CdTe, CIGS, and thin-film Si. Recycling systems have been set up for commercial CdTe modules, which is particularly important because of the use of the toxic element Cd; scarcity of Te is also a concern.

***Methyl-ammonium-lead-halide perovskite (21.0%)***

Hybrid organic-inorganic perovskite solar cells have recently taken the PV research world by storm, with efficiencies above 20% achieved after only 5 years of significant work. These materials have the general formula $ABX_3$, where A is an organic cation (most often methylammonium, $CH_3NH_3$), B is an inorganic cation (usually Pb) and X is a halide (typically I, often with a small fraction of Cl or Br: $CH_3NH_3Pb(I,Cl,Br)_3$). Depending on the halide used, the band gap can be continuously tuned from about 1.6 eV (pure I) to 3.2 eV (pure Cl), with the smaller band gap materials providing better solar cell efficiencies (*25*). Even smaller band gaps can be achieved using a different organic (e.g.

formamidinium, $H_2NCHNH_2$) or inorganic (e.g. Sn) cation, and are desirable as they have a higher efficiency limit (Fig. 1b).

The perovskite salts form polycrystalline films with a perovskite structure at or near room temperature by precipitation from a variety of polar solvents (commonly dimethyl formamide or dimethyl sulfoxide). The device geometry is usually very similar to, and inspired by, those used for solid-state dye-sensitized or polymer bulk-heterojunction solar cells. Typically, an FTO-coated glass substrate is coated with an electron selective contact (usually $TiO_2$). Subsequently, the perovskite is deposited either by spincoating the soluble precursors (methyl ammonium iodide and lead iodide, bromide or chloride) or evaporating the constituent powders. A low-temperature annealing process (<150 °C) often helps improve crystallinity, film morphology and device performance. Finally, the hole-selective top contact (usually Spiro-OMeTAD, $C_{81}H_{68}N_4O_8$) is spincoated on top and the back contact (usually gold) is evaporated to finish the device (Fig. 4h).

The record perovskite solar cell efficiency is 21.0% (*9, 26*)) although for the purpose of this review we analyze cells with the previous record of 20.1% (*9, 26*) as detailed data for the new record cell are not yet available. This (very small-area) cell has the smallest voltage loss among all polycrystalline solar cells ($v$=0.83), even better than the record monocrystalline Si homojunction cells, which is remarkable for a solution-processed semiconductor. Even though the absorption spectrum of perovskites shows a very sharp onset, comparable to the best semiconductor absorbers (CdTe and GaAs), the photocurrent loss is still substantial ($j$=0.88). This loss comes primarily from parasitic absorption in the hole-conducting layer and the back reflector. The fill factor in these cells (*FF*=0.73; $f$=0.81) is the lowest of all cells with efficiencies >20%, most likely due to a combination of non-uniformity (e.g. pinholes) in the absorber and carrier selective contacts that lead to carrier shunting, along with resistive losses associated with non-ideal carrier selective contacts. The fill factor (and thus efficiency) is expected to continue to increase as these factors are optimized further.

Despite the excellent initial performance, hybrid perovskite solar cells are known to degrade within a few hours to days under standard operating conditions, which presently is the greatest barrier to commercial implementation. The origins of perovskite cell instability are currently a topic of active research although photoreduction by ultraviolet light and reactions with water have already been identified as likely candidates. Also, measurements of the current-voltage characteristics can suffer from hysteresis, making efficiency analysis complex. The origin of this hysteresis is still unclear but the leading hypothesis involves ion (or vacancy) migration under operating conditions. As the perovskite salts are partially soluble in water, the cells are sensitive to humidity. Encapsulation and recycling are important (like in the case for CdTe), in view of the toxic Pb, for this technology to become viable for large-scale application. The toxicity challenge is greater for this material than for CdTe and GaAs because the much higher water solubility and lower vaporization temperature make

environmental exposure during module encapsulation failure (breakage, fire) more dangerous. Large band-gap perovskites may serve as a top-cell in Si/perovskite tandem solar cells that have a potential efficiency above 30%; such an application provides a possible entry point to the market for the perovskite technology and is currently under intense research.

***CZTS (12.6%)***

$Cu(Zn,Sn)(S,Se)_2$ ("CZTS") is a solar cell material similar to CIGS, but with the scarce element In replaced with Zn, and Ga replaced with Sn. CZTS can crystalize to form either kesterite or stannite, with kesterite being preferable for photovoltaic applications. As in CIGS, the band gap of CZTS can be tuned over a substantial range (1.0-1.6 eV), with the best results achieved for a Cu-poor, Zn-rich stoichiometry with the band gap controlled by the S/Se ratio.(*27*) The cell structure is nearly identical to what is used for CIGS. Cell fabrication can also follow a similar process, although the record CZTS cells have been made using solution deposition of chalcogenides dissolved in hydrazine followed by annealing in selenium vapor. The record CZTS cell has an efficiency of 12.6% (*9, 28*), and suffers from large voltage loss ($v$=0.58) due to recombination at defects in the bulk material and at the charge extraction interfaces. As with CIGS, the complex nature of the material requires study of many different types of defects and careful engineering of the fabrication and device processing to minimize the most detrimental defects. Controlling interfacial reactions at the Mo metal contact is crucial to reduce interfacial recombination and minimize series resistance. Current loss in CZTS cells is comparable to CIGS ($j$=0.81). Finding an alternative back contact with lower optical loss (higher reflectivity) that can withstand the full device processing and maintain low series resistance would be a major breakthrough in the development of CZTS solar cells, although the biggest factor limiting efficiency is the low $V_{oc}$, stemming from the relatively poor material quality.

***Dye-sensitized solar cells (11.9%)***

Dye-sensitized solar cells are a special class of devices as they involve an electrochemical power generation process. In these cells, the absorber is not an extended solid semiconductor but a molecular dye (typically a ruthenium organometallic complex although zinc porphyrin and even purely organic dyes have also given very high efficiencies) that is coated onto a highly porous nanostructured electrode (typically $TiO_2$). The photoexcited dye injects electrons into the conduction band of the $TiO_2$ and accepts electrons from a redox couple (typically $I^-/I^{3-}$ but higher voltages have been reached with Co-based redox couples) in a non-aqueous electrolyte. The redox active species must then diffuse to the counter electrode (usually Pt or graphite) to be regenerated and complete the current circuit. Dye-sensitized solar cells are made by depositing a very thin compact $TiO_2$ layer

typically on FTO, followed by formation of mesoporous $TiO_2$ by printing a $TiO_2$ nanoparticle paste, annealing, $TiCl_4$ treatment to passivate surface traps, and finally dye adsorption by immersion in solution. A glass plate covered with the counter electrode is brought very close to the substrate using spacers and the cell is filled with electrolyte and sealed. We analyze these cells here using the S-Q model, noting that this model assumes a semiconductor absorber with an absorption band edge, which is not the case for dye-sensitized cells. The numbers for *v* and *j* then provide a reference relative to a conventional semiconductor with a band gap equal to the peak of the dye absorption spectrum (1.50 eV).

The record dye-sensitized cell has an efficiency of 11.9% (*9, 29*) with a large voltage loss (*v*=0.60) due to the relatively low potential of the standard $I^-/I^{3-}$ redox couple which introduces a large energy loss when transferring electrons to the dye. No better dye-based alternatives have been found despite intense research over the past several years: redox couples with higher potentials so far either react too quickly with electrons injected into the $TiO_2$ (leading to recombination) or are too bulky for rapid ionic diffusion through the electrolyte (leading to strong losses in the fill factor at high light levels).

An additional challenge for dye-sensitized solar cells is the relatively high energy and narrow band width associated with molecular absorption, which makes it difficult to harvest a wide range of the solar spectrum (*j*=0.78). Using multiple dyes introduces complications with the redox chemistry while using dyes with broader spectra reduces oscillator strength and requires porous electrodes to become too thick for efficient charge extraction. Despite these difficulties, dye-sensitized solar cells have already been commercialized because of their relatively simple fabrication, low-cost materials and availability in a variety of colors and opacities that are useful when aesthetics are important. Moreover, dye-sensitized solar cells have served as a model system or inspiration for the development for a new class of nanostructured device architectures for photovoltaic solar energy conversion and solar fuel generation.

***Organic solar cells (11.5%)***

Organic solar cells promise cheap, roll-to-roll fabrication on flexible substrates and a wide choice of materials for applications where flexibility and color are important. Organic solar cells come in two varieties: sublimed small-molecule solar cells and solution-processed polymer/fullerene solar cells. The highest reported certified efficiency for a single-junction organic solar cell is 11.5% (*30, 31*), although for the purpose of this review we analyze cells with the previous record of 11.0% (*9, 32*), as detailed data for the new record cell are not yet available. The previous record was achieved using a 1.66 eV-bandgap polymer.

Polymer solar cells are typically prepared on ITO-coated glass or foil with the active polymer-donor/fullerene-acceptor blend sandwiched between a hole selective layer (typically poly(3,4-ethylenedioxythiophene) polystyrene sulfonate ("PEDOT:PSS") or $MoO_3$) and an electron selective layer such as ZnO, $TiO_2$ or a low-work function material such as Ca. The typical active layer thickness is around 100 nm.

Due to the low dielectric constant of organic materials, photo-generated electron-hole pairs remain tightly bound, necessitating the use of dedicated architectures such as bulk heterojunctions to achieve efficient charge separation and extraction. The energy offsets needed for the heterojunction to ensure efficient exciton dissociation lead to a ~0.3 eV voltage loss in practice, which lowers the efficiency by about 2 % absolute (*33*). Currently, the limiting problems for organic solar cells are the high rate of non-radiative recombination via trap states or triplet excited states, and the large degree of static and dynamic disorder, together yielding very high voltage loss ($v$=0.57). To a large extent, this voltage loss could be overcome by direct optical excitation of the charge transfer state between electron donor and electron acceptor. So far, common material combinations show a very low oscillator strength of these charge-transfer states, rendering direct optical excitation nearly absent. Significant current loss ($j$=0.82) is due to parasitic absorption by the selective contacts, incomplete absorption by the polymer, as well as incomplete carrier collection due to non-radiative recombination (low mobility and diffusion length).

As with thin-film silicon solar cells, organic PV technology is suffering from the fact that efficiency is becoming an increasingly important driver to reduce the cost of large-area PV systems. Also, organic cells often show degradation under illumination. At the same time, the relative ease of processing, non-toxicity, low weight, potential for low cost, and the possibility to form flexible modules of many different shapes, colors and transparencies, enables applications that may not be achieved with thin-film flexible CIGS, CdTe, or perovskite cells that have much higher efficiency.

***Thin-film silicon (10.1-11.4%)***

Thin-film microcrystalline or nanocrystalline silicon solar cells can be made on a wide range of (flexible) substrates using chemical vapor deposition. Typically, a p-i-n geometry is grown on a ZnO:Al coated textured glass substrate, followed by a ZnO:Al buffer layer and a Ag back contact. The record efficiency is 11.4% (*9, 34*). The relatively slow deposition rate of crystalline Si limits the cell thickness that can be practically achieved to 2-5 μm and the textured substrate often leads to defected growth of the microcrystalline film. As a result of this thickness limitation, light with energies near the band gap is not fully absorbed, leading to a very strong current penalty with $j$=0.67, the lowest value of all

cells reviewed here. Crystal grain boundaries and other defects in deposited micro/nano-crystalline Si cells are strong sinks for minority carriers, leading to a high voltage loss as well ($v$=0.61).

Amorphous Si (a-Si:H) is a semiconductor with much stronger optical absorption than crystalline Si, but with a band gap well above the optimum (1.7-1.8 eV). It is made using vacuum-deposition techniques, typically at a much higher rate than micro-/nanocrystalline films. Despite the incorporation of hydrogen in these films to passivate bulk defects, the electronic quality of this material is rather low with a correspondingly high voltage loss ($v$=0.61) for the record single-junction cell (10.2%) (*9, 35*). In a-Si:H cells the optimum efficiency is strongly determined by the trade-off between cell thickness and carrier collection efficiency: a large thickness is required to optimize the capture of incident light, but reduces the carrier collection efficiency if the cell is thicker than the carrier drift/diffusion length, which is typically a few hundred nm; for the record cell $j$=0.78. Amorphous Si cells are most often fabricated in a superstrate configuration using a textured glass substrate coated with ITO as a transparent conductor. This then forms the starting point for the subsequent growth of a-Si:H, ZnO:Al buffer layer and Ag back contact.

With cell efficiency becoming an increasingly important driver to reduce the cost of PV, thin-film Si technology has seen a strong setback in recent years. Yet, the possibility of fabricating flexible modules using a roll-to-roll process provides unique application potential, for example in building architecture. Thin-film Si triple-junction cells in which amorphous and microcrystalline Si cells are stacked on top of each other have shown a record efficiency of 13.4% (*36*).

***Quantum dot solar cells (9.9%)***

Quantum dot (QD) solar cells take advantage of the fact that semiconductor quantum dots can be synthesized using (low-temperature) solution processing, with their band gap tunable by composition and size. The best QD solar cells so far are made using PbS or PbSe QDs as the active layer. The QDs are deposited by spin coating or dip coating and then passivated and functionalized using organic molecules or halide salts. A p-n junction is made in the QD layer using a combination of surface ligands. QD cells are typically made on ITO or FTO-coated glass, using a metal oxide (typically ZnO or $TiO_2$) as an electron-selective contact. Molybdenum oxide and Au or Ag are typically used as the back contact.

The record published efficiency for QD solar cells is 9.9% using PbS QDs with a band gap of 1.4 eV, with an architecture similar to previous work (*37*) The 9.9% cells have very high voltage loss ($v$=0.56), the highest loss of all cells reviewed here, which is attributed to the fact that the QDs have a distribution of sizes which results in a distribution of band gap energies. In addition, a high density of radiative sub-bandgap states and strong non-radiative surface recombination due to the large

surface-to-volume ratio in the quantum dots (diameter ~5 nm) leads to recombination. Inefficient transport of carriers by hopping through the QD film limits the QD film thickness that can be practically used. Together, incomplete absorption and strong recombination contribute to a high current loss ($j$=0.66) (note that in the analysis we use as bandgap of the quantum dots the first excitonic peak in the absorption spectrum; taking a smaller electronic bandgap correspondingly increases $v$ and decreases $j$).

***Beyond the Shockley-Queisser limit***

The Shockley-Queisser detailed-balance model describes the efficiency limit for a single-junction solar cell under "one-sun" illumination. Efficiencies beyond the S-Q limit can potentially be achieved for a single-junction cell by using the process of multiple exciton generation (converting a single photon to multiple excitons, e.g. in quantum dots), up- or down conversion of incident light (to make the incident spectral range better match the semiconductor absorption spectrum), or limiting radiative emission (raising the cell voltage). So far, none of these "third generation" PV concepts has led to an enhanced efficiency record for one of the PV materials described above.

Multijunction solar cells constitute a very broad field of research and are beyond the scope of this review (*39*). The highest reported efficiency under one-sun illumination is 38.8%, for a GaInAs/GaInP/GaAs/AlGaInAs/AlGaInP five-junction tandem geometry (*18*). However, the manufacturing costs of such a complex cell architecture is very high.

Concentrating PV, increasing the solar flux by focusing light on a solar cell, can (linearly) increase $J_{sc}$ and (logarithmically) increase $V_{oc}$, leading to a higher efficiency. This concept is being used in PV systems using macroscale lenses or parabolic mirrors in combination with ultra-high efficiency tandem cells. A record cell efficiency of 46.0% was measured using a GaInP/GaAs/GaInAsP/GaInAs tandem cell under 508-fold concentrated light. Concentrating PV requires a tracking system to follow the sun and requires direct (rather than diffuse) sunlight.

**4. Historic efficiency trends**

There are large historic differences in the rate of efficiency improvement for the different materials discussed above. For example, after over 60 years of research, single-crystalline Si is a mature technology, and in recent years only relatively small gradual efficiency improvements have been achieved. In contrast, the record efficiency for the new perovskite materials has climbed rapidly since the first cells were demonstrated, although cells with these record efficiencies are not yet stable in efficiency.

To illustrate recent trends in cell development, Figure 5 compares present efficiencies with the average annual increase in the absolute efficiency over recent years. Crystalline and multicrystalline Si

have recently shown only gradual absolute efficiency improvements in the range of 0.04-0.09 %/year, the increase in c-Si efficiencies resulting from progress in Si heterojunction cells. The high-efficiency thin-film materials perovskite (2.7 %/year), CdTe (0.9 %/year), and CIGS (0.2 %/year) have continuously made significant steps forward over the past few years.

While these recently demonstrated efficiency increases are no guarantee for improvements in the future, the realization of large yearly increases in materials with remaining room for growth in *v*, *j*, and *f* hints that research efforts have not yet become constrained by fundamental limits, and may raise the efficiency of these materials further. Additional research will tell if the record efficiency of CIGS, CdTe or perovskite cells (now 4-5% below that of Si IBC cells) can exceed that of Si cells. The efficiency record for thin-film GaAs cells has not been broken since 2012; a more recent record is for thin-film III-V dual junction cells (31.6%) (*31*). In the low-efficiency (10-12%) category, quantum dot solar cells (1.3 %/year) and organic solar cells (0.6 %/year) continue to make strong progress. Dye-sensitized cells and CZTS have not reported efficiency improvements since 2012 and 2013, respectively. We note that historically, when materials are developed to the level of commercialization, further efficiency increases are often observed beyond the records first achieved in a research laboratory. For example, the present efficiency records for Si IBC, GaAs, and CdTe cells are realized in manufacturing laboratories.

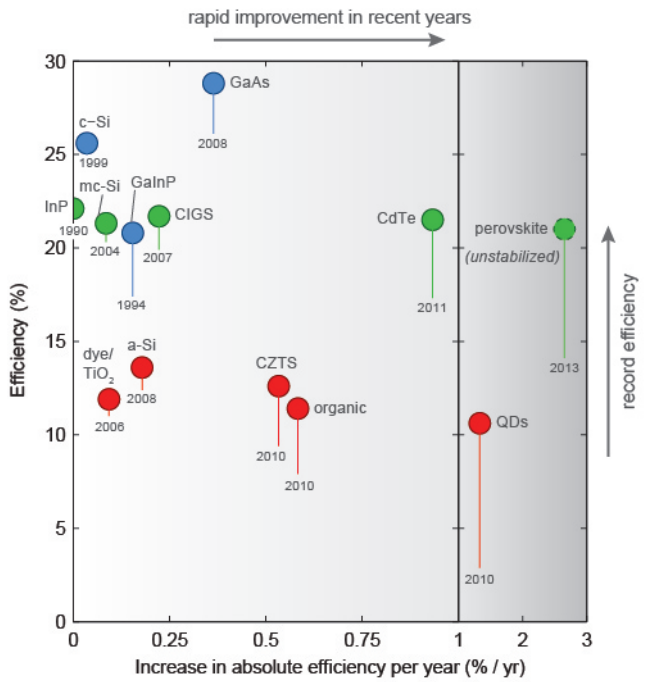


**Figure 5 | Rates of improvement in record solar cell efficiency over recent years.** Average improvements were calculated over a period ending 1-1-2016 and starting with the date of the last record preceding 2010 (with the exception of perovskites: starting 2013, when the first certified efficiency was reported; and CdTe: starting 2011, as no recent record before 2010 was available and much progress occurred after 2010; all years indicated in the figure). Progress in efficiency from the

pre-2010 record to the current values is indicated by the vertical lines. Colors correspond to cells achieving <50% of their S-Q efficiency limit (red), 50-75% (green), or >75% (blue). This analysis is based on data from the NREL efficiency chart, Green's tables, and record cell publications (*11, 20, 31*).

**5. Solar module efficiencies**

Two important factors create a gap between the record efficiency of laboratory solar cells, and the record efficiency of laboratory modules or average efficiency of commercial modules, respectively. First, record cells are the best, often small-area, devices made using specialized laboratory techniques that may be too expensive for large-scale production. For example, thin-film vacuum deposition of metal contacts may be used in the lab, while screen printing of contacts, leading to much lower metal conductivity, is used in the fab. Second, modules are made of a number of larger-area cells connected in series and encapsulated. In the case of wafer-based technologies, incorporation of cells in a module inevitably leads to current losses due to incomplete filling of the module area, and fill factor loss due to additional resistance in cell interconnects and due to the use of larger cells. Optical effects upon encapsulation may decrease or increase efficiency, depending on the specifics of module design. Efficiencies of typical thin-film modules are lower than those of corresponding record cells because of the "dead area" associated with monolithic interconnection of strip-like cells, inhomogeneities or imperfections in the larger areas of the cells, and series resistance because of larger current transport distances.

Furthermore, in practice, solar modules never operate under conditions equal to the standard test conditions (STC). The solar spectrum and intensity change during the day and vary with time of the year. The dependence of efficiency on incident power is generally lowest for cells with high *FF*. Here the high-efficiency (mono)crystalline materials as well as thin-film CIGS and CdTe (all with *FF*>0.79) have an advantage over perovskites and the lower-efficiency thin-film materials (*FF*<0.73*)*. Also, under solar irradiation solar modules heat up, sometimes reducing the efficiency by 1-2% (absolute) compared to their STC value defined at 25$^{o}$C. The temperature coefficient of efficiency depends strongly on material and is lower for Si heterojunction cells, CdTe and CIGS than for other materials (*40, 41*). Another difference between practical, average module efficiency and STC efficiency is related to the fact that in practice modules receive light from a wide range of angles rather than perpendicularly incident light only. This leads to additional reflection losses. Finally we note that nearly all cell/module combinations show reduction in efficiency over time due to a multitude of factors, including degradation of the cells, oxidation of metallic cell interconnects, and photo-degradation of polymer encapsulating layers; the magnitude of these effects depends on the cell/module combination (*42*). Understanding these degradation mechanisms (over the course of 30 years) in different climates is a complex but very important research challenge.

Based on their share in the market for PV systems, which had an estimated value of 96 billion US$ in 2013,(*1*) it can be said that monocrystalline Si, multicrystalline Si, CdTe, and CIGS have evolved into mature high-efficiency technologies, with Si technology having >90% of the market share. Record efficiencies for large-area (>800 $cm^2$) modules are for monocrystalline Si: 22.4% (*9, 43*); multicrystalline Si: 18.5% (*9*), CdTe 18.6%, and CIGS 17.5% (*9, 44*). These materials all belong to the ">75% S-Q limit" (for monocrystalline Si) or "50-75% S-Q limit" (for multicrystalline Si, CIGS, CdTe) classes in Fig. 1b, directly demonstrating the importance of efficiency as a lever for large-scale application.

| **Material** | **Cell eff.** | **Module eff.** | **Technology strengths and options** | **Selected research/technology opportunities** |
|---|---|---|---|---|
| | (%) | (%) | | |
| **Mature technologies deployed at large scale** | | | | |
| monocrystalline Si | 25.6 | 22.4 | earth-abundant material; >25 year track record | further reduce recombination losses, in combination with new metallization schemes; improve light management in thinner wafers; improve IBC and SHJ cell designs |
| multicrystalline Si | 20.8 | 18.5 | earth-abundant material; >25 year track record | improve wafer quality (minimize or passivate defects) to reduce recombination losses |
| CIGS | 21.7 | 17.5 | flexible substrates | improve light management; increase efficiency for large band gaps (tandem cells); reduce recombination losses, solution processing |
| CdTe | 21.5 | 18.6 | flexible substrates; short energy payback time | reduce recombination losses; develop thinner cell designs using light management |
| **Emerging technologies deployed at smaller scale** | | | | |
| dye-sensitized $TiO_2$ | 11.9 | 10.0 | tunable colors | Improve redox couple; reduce recombination losses; increase band gap; increase stability |
| thin-film Si | 11.4 | 12.2* | flexible modules | reduce recombination losses; improve light management |
| organic | 11.5 | 9.5 | flexible modules, semi-transparent modules | improve light management; increase band gap, increase stability; reduce recombination losses |
| **Technology at the manufacturing level** | | | | |
| GaAs | 28.8 | 24.1 | very high efficiency; flexible modules | improve light management; develop IBC geometry; further develop thin-film multijunction cells by layer transfer |
| **Technologies under development** | | | | |
| perovskite | 21.0 | n.a. | solution processing; flexible modules | reduce recombination losses; improve cell stability; avoid use of Pb; increase efficiency for high band gap materials (tandem cells); develop Si/perovskite tandems |
| CZTS | 12.6 | n.a | flexible modules | reduce recombination losses; improve light management |
| quantum dots | 9.9 | n.a. | solution processing; flexible modules | reduce recombination losses; improve light management; avoid use of Pb |

**Table 1 | Technology strengths and key research opportunities for photovoltaic materials**. Materials are grouped by degree of technological development. Record cell and module efficiencies are indicated, based on certified measurements. GaInP and InP are not included as no significant development towards commercial technology exists. *microcrystalline Si/a-Si tandem geometry.

A recent development is the demonstration of single-junction GaAs solar modules with a record efficiency of 24.1% that are fabricated on an industrial scale, and are now on their way to commercial exploitation (*45*). It will be interesting to see how the manufacturing costs for each of the >20% module technologies will decrease in the coming years. Thin-film solar cells deposited on thin foils are also expected to find additional new applications in areas where low weight-specific power (W/g) is desired, and in novel forms of building-integrated photovoltaics where flexible form factors or partial transparency for visible light are desired.

Thin-film amorphous and crystalline silicon modules and flexible foils have also been developed to a commercial level but are applied on a much smaller scale due to their lower efficiency (12.2% for a module based on a tandem geometry) and higher manufacturing costs (*46*). Furthermore, small-area modules of dye-sensitized solar cells (efficiency 10.0%) (*47, 48*) and organic solar cells (9.5%) (*32*) are commercially available but thus far represent a small market. Thin-film perovskite, CZTS and quantum dot solar cells have been demonstrated in the lab but modules have not (yet) been demonstrated on a significant industrial scale. For perovskites the long-term stability and manufacturability still has to be demonstrated, for CZTS and quantum dot solar cells so far the low efficiency limits commercial development. Table 1 summarizes technological strengths and selected research technology opportunities for all reviewed materials.

**6. Large-scale application of PV**

The present worldwide primary energy supply through all sources (fossil, nuclear and renewable) amounts to 18.0 TW; final consumption is 12.3 TW (*49*). In principle, this energy need can be fully met using photovoltaics, in combination with proper energy transport and storage systems and secondary conversion into heat and fuels. Assuming a modest module efficiency of 20%, a system capacity factor of 15%, an average ground cover ratio of 50% and 50% losses related to storage and secondary conversion, 1.6% of the earth's land area would be required to produce an amount of energy equal to the current primary supply. While in absolute terms this is a very large number, it is not unrealistic. To put this in perspective: this area is over 20 times less than the area used for agriculture worldwide worldwide. Also note that significant land areas are already used today for production of fossil fuels and various types of biofuel. Finally, by drastically increasing the efficiency of solar modules, by integrating PV into buildings and other objects, and by combining PV technology with other renewable sources such as solar thermal energy and wind energy, a much smaller area is needed.

For PV to break through at such a large scale, a further reduction in costs of PV technology is required. As stated above, increasing cell efficiency is a key driver for reducing costs, as the costs of the solar cells themselves constitute only part (<50%) of the costs of a full PV system. Furthermore,

overall costs of PV systems will decrease by economy-of-scale as production capacity and installation volumes are further increased. Scalability of technology and availability of raw materials are essential parameters, as are the energy costs of fabricating PV systems at a large scale. Long lifetime and stable operation are additional crucial parameters, as is design-for-recycling, which allows valuable or toxic materials to be recovered in a practical way.

**7. Future research directions: light management and carrier management**

In this review we have categorized 16 photovoltaic materials architectures in terms of their current and voltage loss relative to the S-Q limiting values. To further increase the photocurrent in a particular cell design typically requires better management of light in order to reduce reflection, reduce parasitic absorption and enhance light trapping in the active area of the cell. Nanophotonic concepts, in which nanostructures with typical length scales equal or smaller than the wavelength of light are incorporated in the solar cell, can serve to reach these goals (*5, 50-52*). Such structures can preferentially scatter and confine light so that it is better absorbed in the cell. Nanophotonic concepts leading to enhanced light trapping can also reduce the required material thickness, thereby reducing bulk recombination, which enhances the voltage, and reducing costs. Nanophotonic control can also enhance the voltage reducing entropic losses via control of the angular distribution of light emission from the cell. Large-area engineered nanopatterns, integrated in solar cells, can be made using soft-imprint technology that can be scaled up to the square-km areas required for large-area production. We predict that further advances in nanophotovoltaics will lead to enhanced photocurrents and thus enhanced efficiencies in several different photovoltaic materials and architectures. Nanophotonic concepts can also be used to engineer the color of solar panels, providing many new opportunities for building-integrated photovoltaics.

Improving the cell voltage and fill factor requires detailed understanding of and control over carrier recombination mechanisms in the cell. Making advances in electrical materials quality is a major materials engineering research effort that involves identification of bulk, interface, and surface defects, and measuring their density, energy levels, formation energy, annealing characteristics, passivation behavior, understanding dopant diffusion, contact formation, and many other properties. To realize high-quality photovoltaic materials that lead to solar cells with efficiencies approaching the S-Q limit and that can be made at low costs will require a major man-to-the-moon-type coordinated international materials science and engineering approach.

**8. Conclusions and outlook**

The record efficiency of single-junction solar cells has continuously increased over the years, but so far no photovoltaic material has closely approached the theoretical Shockley-Queisser efficiency limit.

Monocrystalline Si and GaAs have reached efficiencies of 26-29%, several polycrystalline materials (Si, CIGS, CdTe, perovskite) are in the 20-22% range; all other common thin-film materials have efficiencies in the 10-13% range. Based on an analysis of record-cell characteristics for all these materials we reviewed the major loss mechanisms and provided a perspective for improvements in both light management and charge carrier collection for all these materials. There is much room for improvement in all of the materials discussed and there is no doubt that efficiency records will continue to be broken in the future (*30*). The lower-efficiency (flexible) materials can find applications in building-integrated photovoltaic systems, flexible electronics, flexible power generation systems and many other (sometimes niche) markets. High-efficiency (>20%) materials find applications in large-area PV power generation for the utility grid as well as in small and medium-sized systems for the built environment. They will enable very large-scale penetration into our energy system, starting now and growing as the cost/kWh is reduced further by a factor of 2 to 3. This can be achieved by advanced (nanophotonic) cell designs in combination with an extensive materials science and engineering effort to further enhance photovoltaic material quality.

***References***


1. "Technology roadmap: Solar photovoltaic energy (2014 edition)," (International Energy Agency, Paris, France, 2014).
2. W. Shockley, H. J. Queisser, Detailed balance limit of efficiency of p-n junction solar cells. *J. Appl. Phys* **32**, 510-519 (1961).
3. T. Tiedje, Band tail recombination limit to the output voltage of amorphous silicon solar cells. *Appl. Phys. Lett.* **40**, 627-629 (1982).
4. U. Rau, J. H. Werner, Radiative efficiency limits of solar cells with lateral band-gap fluctuations. *Appl. Phys. Lett.* **84**, 3735-3737 (2004).
5. U. Rau, U. W. Paetzold, T. Kirchartz, Thermodynamics of light management in photovoltaic devices. *Phys. Rev. B* **90**, 035211 (2014).
6. M. Topic, R. M. Geisthardt, J. R. Sites, Performance limits and status of single-junction solar cells with emphasis on CIGS. *IEEE J. Photovolt.* **5**, 360-365 (2015).
7. S. W. Glunz *et al.*, "The irresistible charm of a simple current flow pattern - 25% with a solar cell featuring a full-area back contact," Proc. 31st EU PVSEC, Hamburg, Germany, 15 Sept. 2015.
8. J. Zhao, A. Wang, M. A. Green, F. Ferrazza, 19.8% efficient “honeycomb” textured multicrystalline and 24.4% monocrystalline silicon solar cells. *Appl. Phys. Lett.* **73**, 1991-1993 (1998).
9. M. A. Green, K. Emery, Y. Hishikawa, W. Warta, E. D. Dunlop, Solar cell efficiency tables (version 45). *Prog. Photovolt.* **23**, 1-9 (2015).
10. P. J. Cousins *et al.*, "Gen III: Improved performance at lower cost," Proc. 35th IEEE PVSC, Honolulu, HI, June 2010.
11. M. A. Green, K. Emery, Y. Hishikawa, W. Warta, E. D. Dunlop, Solar cell efficiency tables (version 47). *Prog. Photovolt.* **24**, 3-11 (2016).
12. Panasonic press release: Panasonic HIT® solar cell achieves world's highest energy conversion efficiency of 25.6% at research level (Apr. 24, 2014). http://news.panasonic.com/press/news/official.data/data.dir/2014/04/en140410-4/en140410-4.html.

13. P. Verlinden *et al.*, "Strategy, development, and mass production of high-efficiency crystalline Si PV modules", paper presented at the 6th World Conf. on PV Energy Conversion, Kyoto, Japan, 2014.
14. A. Richter, M. Hermle, S. W. Glunz, Reassessment of the limiting efficiency for crystalline silicon solar cells. *IEEE J. Photovolt.* **3**, 1184-1191 (2013).
15. D. D. Smith *et al.*, "Generation III high efficiency lower cost technology: Transition to full scale manufacturing," Proc. 38th IEEE PVSC, Austin, TX, 3-8 June 2012.
16. B. M. Kayes *et al.*, "27.6% conversion efficiency, a new record for single-junction solar cells under 1 sun illumination," Proc. 37th IEEE Photovolt. Specialists Conf., Seattle, WA, 19-24 June 2011.
17. E. D. Kosten, J. H. Atwater, J. Parsons, A. Polman, H. A. Atwater, Highly efficient GaAs solar cells by limiting light emission angle. *Light: Sci. Appl.* **2**, e45 (2013).
18. P. T. Chiu *et al.*, "35.8% space and 38.8% terrestrial 5j direct bonded cells," Proc. 40th IEEE PVSC, Denver, CO, 8-13 June 2014.
19. C. J. Keavney, V. E. Haven, S. M. Vernon, "Emitter structures in MOCVD InP solar cells," Proc. 21st IEEE PVSC, Kissimmee, FL, 21-25 May 1990.
20. J. F. Geisz, M. A. Steiner, I. Garcia, S. R. Kurtz, D. J. Friedman, Enhanced external radiative efficiency for 20.8% efficient single-junction GaInP solar cells. *Appl. Phys. Lett.* **103**, 041118 (2013).
21. S. Essig *et al.*, Realization of GaInP/Si dual-junction solar cells with 29.8 percent one-sun efficiency. *unpublished*.
22. P. Jackson *et al.*, Properties of Cu(In,Ga)Se2 solar cells with new record efficiencies up to 21.7%. *Phys. Status Solidi RRL* **9**, 28-31 (2015).
23. First solar press release: First solar achieves efficiency, durability milestones (Feb. 5, 2015). http://investor.firstsolar.com/releasedetail.cfm?ReleaseID=895118.
24. First solar press release: First solar builds the highest efficiency thin film PV cell on record (August 5, 2014). http://investor.firstsolar.com/releasedetail.cfm?ReleaseID=864426.
25. G. Xing *et al.*, Low-temperature solution-processed wavelength-tunable perovskites for lasing. *Nature Mater.* **13**, 476-480 (2014).
26. N. J. Jeon *et al.*, Compositional engineering of perovskite materials for high-performance solar cells. *Nature* **517**, 476-480 (2015).
27. T. K. Todorov, K. B. Reuter, D. B. Mitzi, High-efficiency solar cell with earth-abundant liquid-processed absorber. *Adv. Mater.* **22**, E156-E159 (2010).
28. W. Wang *et al.*, Device characteristics of CZTSSe thin-film solar cells with 12.6% efficiency. *Adv. Energy Mater.* **4**, 1301465 (2014).
29. R. Komiya *et al.*, "Improvement of the conversion efficiency of a monolithic type dye-sensitized solar cell module," Technical digest, 21st PVSEC, Fukuoka, Japan, Nov. 2011.
30. An overview of all records with updated values for current and voltage relative to the Shockley-Queisser limits (table S1) is kept up to date on www.amolf.nl/lmpv/SQ.
31. NREL, Research cell efficiency records. http://www.nrel.gov/ncpv/images/efficiency_chart.jpg (accessed: Feb. 11, 2016).
32. M. Hosoya *et al.*, "Module development for polymer solar cells," Proc. Grand Renewable Energy Conference, Tokyo, Japan, Aug. 2014.
33. T. Kirchartz, K. Taretto, U. Rau, Efficiency limits of organic bulk heterojunction solar cells. *J Phys Chem C* **113**, 17958-17966 (2009).
34. H. Sai, T. Matsui, K. Matsubara, M. Kondo, I. Yoshida, 11.0%-efficient thin-film microcrystalline silicon solar cells with honeycomb textured substrates. *IEEE J. Photovolt.* **4**, 1349-1353 (2014).
35. T. Matsui *et al.*, "Development of highly stable and efficient amorphous silicon based solar cells," Proc. 28th EU PVSEC, Paris, France, Sept. 2013.
36. S.-W. Ahn, S.-E. Lee, H. M. Lee, "Toward commercialization of triple-junction thin-film silicon solar panel with >12% efficiency", paper presented at the Proc. 37nd PVSEC Conference, Frankfurt, Germany, Sept. 2012.

37. C.-H. M. Chuang, P. R. Brown, V. Bulovic, M. G. Bawendi, Improved performance and stability in quantum dot solar cells through band alignment engineering. *Nature Mater.* **13**, 796-801 (2014).
38. Fraunhofer Institute press release: New world record for solar cell efficiency at 46% (December 1, 2014). https://www.ise.fraunhofer.de/en/press-and-media/press-releases/press-releases-2014/new-world-record-for-solar-cell-efficiency-at-46-percent.
39. K. Tanabe, A review of ultrahigh efficiency III-V semiconductor compound solar cells: Multijunction tandem, lower dimensional, photonic up/down conversion and plasmonic nanometallic structures. *Energies* **2**, 504-530 (2009).
40. A. Virtuani, D. Pavanello, G. Friesen, "Overview of temperature coefficients of different thin film photovoltaic materials," Proc. 25th EU PVSEC, Valencia, Spain, 6-10 Sept. 2010.
41. T. Mishima, M. Taguchi, H. Sakata, E. Maruyama, Development status of high-efficiency HIT solar cells. *Sol. Energy Mater. Sol. Cells* **95**, 18-21 (2011).
42. R. Jones-Albertus, D. Feldman, R. Fu, K. Horowitz, M. Woodhouse, Technology advances needed for photovoltaics to achieve widespread grid price parity. *Unpublished*, (2016).
43. R. Swanson, "The role of modeling in sunpower's commercialisation efforts", paper presented at the Workshop on Challenges in PV science, technology, and manufacturing, Purdue University, West Lafayette, IN, Aug. 2012.
44. H. Sugimoto, "High efficiency and large volume production of CIS-based modules," Proc. 40th IEEE PVSC Denver, CO, June 2014.
45. H. Sai *et al.*, Microcrystalline silicon solar cells with 10.5% efficiency realized by improved photon absorption via periodic textures and highly transparent conductive oxide. *Appl. Phys. Expr.* **6**, 104101 (2013).
46. Tel solar press release (July 9 , 2014).
47. H. Ozawa, Y. Okuyama, H. Arakawa, Dependence of the efficiency improvement of black-dye based dye-sensitized solar cells on alkyl chain length of quaternary ammonium cations in electrolyte solutions. *Chem. Phys. Chem.* **15**, 1201-1206 (2014).
48. N. Tanabe, Dye sensitized solar cell for energy harvesting applications. *Fujikura Technical Review*, 109-113 (2013).
49. "Key world energy statistics," (International Energy Agency (IEA), Paris, France, 2015).
50. H. A. Atwater, A. Polman, Plasmonics for improved photovoltaic devices (vol 9, pg 205, 2010). *Nature Mater.* **9**, 865-865 (2010).
51. M. L. Brongersma, Y. Cui, S. H. Fan, Light management for photovoltaics using high-index nanostructures. *Nature Mater.* **13**, 451-460 (2014).
52. A. Polman, H. A. Atwater, Photonic design principles for ultrahigh-efficiency photovoltaics. *Nature Mater.* **11**, 174-177 (2012).
53. J. L. Shay, Photoreflectance line shape at the fundamental edge in ultrapure GaAs. *Phys. Rev. B* **2**, 803-807 (1970).
54. W. Bludau, A. Onton, W. Heinke, Temperature dependence of the band gap of silicon. *J. Appl. Phys* **45**, 1846-1848 (1974).
55. L. Pavesi, F. Piazza, A. Rudra, J. F. Carlin, M. Ilegems, Temperature-dependence of the InP band-gap from a photoluminescence study. *Phys. Rev. B* **44**, 9052-9055 (1991).
56. D. Weiwei *et al.*, 20.8% perc solar cell on 156 mm × 156 mm p-type multicrystalline silicon substrate. *IEEE J. Photovolt.* **6**, 3-9 (2016).
57. M. A. Green, K. Emery, Y. Hishikawa, W. Warta, E. D. Dunlop, Solar cell efficiency tables (version 41). *Prog. Photovolt.* **21**, 1-11 (2013).
58. H. Helmers, C. Karcher, A. W. Bett, Bandgap determination based on electrical quantum efficiency. *Appl. Phys. Lett.* **103**, 032108 (2013).

**Acknowledgements**

This work is part of the research program of the Foundation for Fundamental Research on Matter (FOM), which is part of the Netherlands Organisation for Scientific Research (NWO). It is also supported by NanoNextNL, a nanotechnology program of the Dutch ministry of economic affairs, the European Research Council (ERC), and the Global Climate and Energy Project (GCEP). The authors declare no competing financial interests. The data are archived in the laboratory of A.P. The data in Table S1 will be continuously updated and made available on www.amolf.nl/lmpv/SQ.

**Supplementary material**

| Material | tf/w | Lab/company | Eff. | $J_{sc}$ | *Voc* | *FF* | *j* | *v* | *f* | $E_g$ | Ref. | |
|---|---|---|---|---|---|---|---|---|---|---|---|---|
| | | | (%) | ($mAcm^{-2}$) | (mV) | | $J_{sc}/J_{SQ}$ | $V_{oc}$ / $V_{SQ}$ | FF / $FF_{SQ}$ | (eV) | Cell | $E_g$ |
| GaAs | tf | Alta Devices | 28.8 | 29.7 | 1.122 | 0.865 | 0.92 | 0.97 | 0.97 | 1.42 | (*16*) | (*53* ) |
| Si SHJ/IBC | w | Panasonic | 25.6 | 41.8 | 0.740 | 0.827 | 0.96 | 0.84 | 0.95 | 1.12 | (*12*) | (*54* ) |
| Si IBC | w | SunPower | 25.0 | 41.5 | 0.726 | 0.828 | 0.95 | 0.83 | 0.95 | 1.12 | (*10*) | (*54*) |
| Si TOPCon | w | Fraunhofer | 25.1 | 42.1 | 0.718 | 0.832 | 0.96 | 0.82 | 0.96 | 1.12 | (*7*) | (*54*) |
| GaInP | w | NREL | 20.8 | 16.0 | 1.455 | 0.893 | 0.82 | 0.96 | 0.98 | 1.81 | (*20*) | (*20*) |
| InP | w | Spire | 22.1 | 29.5 | 0.878 | 0.854 | 0.85 | 0.81 | 0.96 | 1.35 | (*19*) | (*55*) |
| CuInGaSe/S | tf | ZSW Stuttgart | 21.7 | 36.5 | 0.748 | 0.794 | 0.84 | 0.84 | 0.91 | 1.13 | (*22*) | (*22*) |
| multicryst. Si | w | Trina Solar | 21.3 | 39.8 | 0.668 | 0.803 | 0.91 | 0.76 | 0.92 | 1.12 | (*11, 56*) | (*54*) |
| CdTe | tf | First Solar | 21.0 | 30.3 | 0.876 | 0.794 | 0.96 | 0.75 | 0.89 | 1.43 | (*24*) | (*9*)* |
| perovskite | tf | KRICT | 20.1 | 22.5 | 1.100 | 0.732 | 0.88 | 0.83 | 0.81 | 1.60 | (*26*) | (*26*)* |
| CuZnSnSe/S | tf | IBM | 12.6 | 35.2 | 0.513 | 0.698 | 0.81 | 0.58 | 0.80 | 1.13 | (*28*) | (*28*) |
| dye/$TiO_2$ | tf | Sharp | 11.9 | 22.5 | 0.744 | 0.712 | 0.78 | 0.60 | 0.79 | 1.50 | (*29*) | (*57*)* |
| nanocryst. Si | tf | AIST | 11.4 | 29.1 | 0.535 | 0.731 | 0.67 | 0.61 | 0.84 | 1.12 | (*34*) | (*54* ) |
| organic | tf | Toshiba | 11.0 | 19.4 | 0.793 | 0.714 | 0.82 | 0.57 | 0.79 | 1.66 | (*32*) | (*9*) |
| amorphous Si | tf | AIST | 10.2 | 16.4 | 0.896 | 0.698 | 0.78 | 0.61 | 0.76 | 1.76 | (*35*) | (*9*)* |
| quantum dots | tf | U Toronto | 9.9 | 21.6 | 0.635 | 0.719 | 0.66 | 0.56 | 0.80 | 1.40 | (*37*) | (*37*) |

**Table S1 | Performance parameters for record solar cells**. Cells are grouped by the fraction of the S-Q detailed-balance efficiency limit achieved: >75% (blue), 50-75% (green), and <50% (red). tf=thin-film, w=wafer-based solar cell. *j, v,* and *f* are the short-circuit current, open-circuit voltage and fill factors normalized to maximum values according to the S-Q model: , $j=J_{sc}/J_{SQ}$, $v=V_{oc}/V_{SQ}$, $f=FF/FF_{SQ}$ using the listed band gap energies. Record efficiencies were all taken from Refs. (*9, 11*) except for dye/$TiO_2$ (ref. (*57*)) and quantum dots (Ref. (*37*)). Details on each record cell are given in the references under Ref.-Cell; references for the band gaps $E_g$ used in the S-Q analysis are given under Ref.-$E_g$. *Indicates that $E_g$ was derived from external quantum efficiency data in that reference using the method in Ref. (*58*); the fitting process yields an uncertainty on the order of ±10 meV. While new certified records have been reported for CdTe (21.5%, First Solar) (*23*), perovskite (21.0% EPFL (*9*)) and organic solar cells (11.5%, Hong Kong University), they are not analyzed here because detailed data are not yet available. Record cell efficiencies were measured for cells with an area >1 $cm^2$, with the exception of GaInP, CIGS, CZTS and perovskite (*9*). For updated values, see: www.amolf.nl/lmpv/SQ.

REVIEW SUMMARY

PHOTOVOLTAICS

# Photovoltaic materials – present efficiencies and future challenges

Albert Polman[1]*, Mark Knight[1], Erik C. Garnett[1], Bruno Ehrler[1], and Wim C. Sinke[1,2]

**BACKGROUND:** Photovoltaics (PV), which directly convert solar energy into electricity, offer a practical and sustainable solution to the challenge of covering the increasing global energy demand. According to the Shockley-Queisser (S-Q) detailed-balance model, the limiting photovoltaic energy conversion efficiency for a single-junction solar cell is 33.7 %, for an optimum semiconductor band gap of 1.34 eV. Parallel to the development of wafer-based Si solar cells, for which the record efficiency has continuously increased over the last decades, a large range of thin-film materials have been developed with the aim to approach the S-Q limit. These materials can potentially be deposited at low cost, in flexible geometries, and using relatively small material quantities.

**ADVANCES**: We review the electrical characteristics of record cells illuminated under the standard AM1.5 solar spectrum made from the 16 widely studied photovoltaic materials geometries and compare these to the fundamental limits based on the S-Q model. Cells that show a short-circuit current ($J_{sc}$) lower than the S-Q limit suffer from incomplete light absorption or incomplete collection of generated carriers, while a reduced open circuit voltage ($V_{oc}$) or fill factor (*FF*) reflects unwanted bulk or interfacial carrier recombination, parasitic resistance, or other electrical non-idealities. The figure shows the experimental values for $J_{sc}$ and the $V_{oc}$×*FF* product relative to the S-Q limiting values for the different materials. This graph enables a direct identification of each material in terms of unoptimized light management and carrier collection ($J_{sc}/J_{SQ} < 1$) or carrier management ($V_{oc}$×*FF*/$V_{SQ}$×$FF_{SQ} < 1$).

The figure shows that monocrystalline Si cells (record efficiency 25.6%) have reached near-complete light trapping and carrier collection, and are mostly limited by remaining carrier recombination losses. In contrast, thin-film single-crystalline GaAs cells (28.8%) show only minimal recombination losses, but can improve by better light management. Polycrystalline CdTe thin film cells (21.5%) show excellent light absorption but relatively high recombination losses; perovskite (21.0%) and CIGS (21.7%) cells show poorer light management, respectively, but CIGS shows higher electrical quality..

Aside from these five high-efficiency materials (Si, GaAs, CdTe, CIGS, perovskite, all >20%), a broad range of other thin film materials have been developed, with efficiencies that are so far limited to 10-12%: micro/nanocrystalline and amorphous Si, CZTS, dye-sensitized $TiO_2$, organic/polymer materials, and quantum dot solids. So far, cell designs based on these materials all suffer from both light management and carrier management problems. Organic and quantum dot solar cells are continuously showing significant efficiency improvements in recent years.

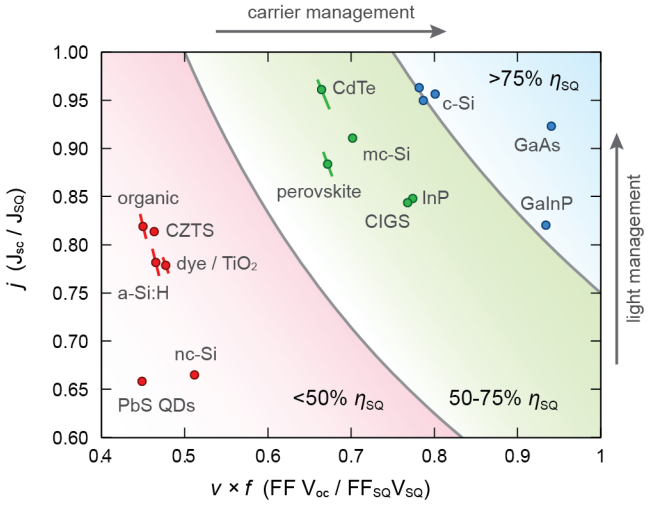


**Limiting processes in photovoltaic materials.** An efficient solar cell captures and traps all incident light ("light management") and converts it to electrical carriers that are efficiently collected ("carrier management"). The plot shows the short-circuit current and product of open-circuit voltage and fill factor relative to the maximum achievable values, based on the Shockley-Queisser detailed-balance limit, for the record-efficiency solar cell made with each photovoltaic material. The data indicate whether a particular material requires better light management, carrier management or both. Colors correspond to cells achieving <50% of their S-Q efficiency limit (red), 50-75% (green), or >75% (blue).

**OUTLOOK:** The record-efficiency single-crystalline materials (Si, GaAs) have room for efficiency improvements by a few absolute percent. The future will tell if the high-efficiency polycrystalline thin films (CdTe, CIGS, perovskite) can rival the efficiencies of Si and GaAs. As the cost of photovoltaic systems is only partly determined by the cost of the solar cells, efficiency is a key driver to reduce the cost of solar energy, and therefore large-area photovoltaic systems require high-efficiency (>20%), low cost, solar cells. Low-efficiency (10-12%) thin film materials will find applications in markets where cost per kWh is not the key determining factor, such as in building-integrated photovoltaic systems, flexible electronics, flexible power generation systems and many other (sometimes niche) markets.

---

[1]Center for Nanophotonics, FOM Institute AMOLF, Science Park 104, 1098 XG Amsterdam, the Netherlands; [2]Energy research Center of the Netherlands (ECN), P.O. Box 1, Petten, the Netherlands.
[*]Corresponding author. E-mail: polman@amolf.nl